Iran J Pharm Res. 2022 December; 21(1):e123824. doi: 10.5812/ijpr.123824.

Published online 2022 February 17. **Research Article**

Preparation and Characterization of Nanosuspensions of Triiodoaniline Derivative New Contrast Agent, and Investigation into Its Cytotoxicity and Contrast Properties

Mehmet Koca [#1], Rukiye Sevinç Özakar [#2,*], Emrah Ozakar [2], Recep Sade [2], Berhan Pirimoğlu [3], Nihal Şimsek Özek [4] and Ferhunde Aysin [4]

[1]Department of Pharmaceutical Chemistry, Faculty of Pharmacy, Atatürk University, Erzurum, Turkey
[2]Department of Pharmaceutical Technology, Faculty of Pharmacy, Atatürk University, Erzurum, Turkey
[3]Department of Radiology, Faculty of Medicine, Atatürk University, Erzurum, Turkey
[4]Department of Biology, Faculty of Science, Atatürk University, Erzurum, Turkey

[*]*Corresponding author*: Department of Pharmaceutical Technology, Faculty of Pharmacy, Atatürk University, Erzurum, Turkey. Email: rukiyeso@atauni.edu.tr
# These authors are contributed equally as the first author.

Received 2021 September 10; **Revised** 2021 November 23; **Accepted** 2021 November 24.

Abstract

Iodine-based contrast agents have limitations such as rapid clearance, potential renal toxicity, non-specific blood pool distribution, headache, and adverse events. Nowadays, it is quite common to work with nanosized systems in order to eliminate the side effects of contrast agents. This study aims to synthesize a new iodinated contrast agent, prepare its nanosuspension by using the nanoprecipitation method, investigate its cytotoxicity, and compare its contrast properties with iohexol and iopromide through in-vitro experiments. The values of nanosuspension particle size and zeta potential have been found to be ~ 400 nm and ~ (-) 15 mV, respectively. In-vitro cellular viability findings indicated that the nanosuspension has lower cytotoxicity than the iohexol and iopromide. In the computed tomography (CT) imaging study of contrast features of nanosuspensions and two commercial agents, which involved 86 CT examinations using 31 parameters and two different devices, it was found that iodine had a stronger presence in its nanosuspension form than in iohexol and iopromide, which were the other two commercial contrast agents, when used in equal amounts. Thus in the case of nanosuspensions contrast brightness was achieved by using less iodine, while the same brightness could be obtained with higher doses of iohexol and iopromide. CT imaging therefore be done without much chemical use, which indicates that it may witness fewer side effects in the future.

Keywords: Radiocontrast Agent, CT Imaging, Cytotoxicity, Nanosuspension, Synthesis, Viscosity, Stability

1. Background

Compounds that absorb X-rays and cause a significant contrast in films are called X-ray contrast agents. X-ray contrast agents must have high density and atomic numbers to obtain high-quality imaging. Such contrast agents must contain molecules with high X-ray attenuation (image contrast) quality. Currently, iodine-based contrast agents are often used because of their high atomic number (Z = 53) and X-ray attenuation properties for medical imaging purposes. In CT, image contrast depends on photoelectric absorption, which is affected by the atomic number of the matter. As iodine has a high atomic number, compared to most tissues in the body, the administration of iodinated material produces image contrast due to differential photoelectric absorption (1, 2). The absorption and scattering of X-ray radiation of iodine-based contrast agents in the target organs or blood vessels are more significant than those of the other contrast agents (3). Monomeric agents have a tri iodinated benzene ring, and dimeric agents have two tri-iodinated benzene rings. They can be classified as ionic and non-ionic contrast agents in accordance with their solubility in water (4). Ionic contrast agents have more of disadvantages than non-ionic contrast agents do. Ionic agents tend to interact with biological structures such as peptides and cell membranes. Due to their high toxicity, the use of ionic contrast agents has been limited in recent years (1, 4). These drugs can cause acute kidney failure, and this possibility increases more in advanced age and in cases of diabetes and chronic kidney disease (5). Also, general limitations of iodinated contrast agents comprise fast clearance, potential renal toxicity, non-specific blood pool distribution, vomiting, headache,

and adverse events/anaphylaxis (2, 6). Iohexol and iopromide are widely used as water-soluble non-ionic contrast agents with monomeric structures (4).

Studies on nanosized systems have recently assumed great significance as these systems can eliminate the side effects of contrast agents used today. Different approaches and formulations are being studied to develop nanosized contrast agents, including nanoemulsions, microspheres, liposomes, micelles, and polymeric nanoparticles (1). About 60% of newly synthesized drug molecules exhibit disordered absorption with a water-insoluble or slightly water-soluble structure. Thus, they require new formulations and drug delivery systems. Nanosuspensions offer an alternative and promising universal formulation approach, which increases the efficacy and the pharmacoeconomics of most of the drugs. Nanosuspension technology improves drug safety and efficacy by changing the solubility and the pharmacokinetics of a drug (7). Nanosuspensions are generally stabilized with surfactants or polymeric steric stabilizers and contain 100% pure drug particles without a carrier system or delivery vehicle. Thus, they are a completely different pharmaceutical technology with different manufacturing techniques compared to polymeric drug delivery systems. Owing to its high drug content, nanosuspension technology can help to efficiently transport the drug entering the cells at a high rate, achieve sufficiently high therapeutic concentrations, and maximize pharmacological effects.

Numerous studies have proved the feasibility and efficiency of this technology for drug delivery. For example, in various studies, the nanosuspension form has been found to be an excellent drug delivery system for cancer treatment with increased antitumor efficacy and reduced toxicity for water-insoluble drugs in relation to common commercial preparations. In nanosuspension studies, it has been emphasized that the size and distribution of the particles, their morphology and, crystalline state, stabilizers, and application routes are key factors affecting nanosuspension efficiency and bioavailability in nanosuspension studies (8). Nanomedicine studies have found increasing use of nanoparticles in various medical imaging techniques such as PET, MRI, photoacoustic, and fluorescence imaging. Generally, nanoparticles carry a high amount of contrast materials and, therefore, there are many exciting applications of contrast agent-loaded nanoparticles for CT (2, 9). Nanoparticles help reduce the side effects of drugs that cause toxicity in conventional ways. Designing a functional nanoparticle makes it possible to create an imaging function for it (10).

In this study, a practical method was used first to synthesize a new triiodoaniline derivative "4-nitro-N-(2,4,6-triiodophenyl) benzamide" (4N-TIB) with a high yield. The authors aimed to prepare nanosuspensions of a water-insoluble 4N-TIB molecule, investigate its cytotoxicity, and compare its contrast properties with contrast agents currently used in CT imaging.

2. Methods

2.1. Materials

Dioxane and hydrogen peroxide used in the synthesis were purchased from Merck and; iodine and 4-nitrobenzoyl chloride from Sigma-Aldrich. Dimethyl sulfoxide (DMSO) and polyvinyl alcohol (PVA) (MW 130000, 99% hydrolyzed) used in nanosuspension preparation were sourced from Honeywell and Sigma-Aldrich. The chemicals used in the cell culture study: Dulbecco's modified Eagle's medium (DMEM) and antibiotic solution of penicillin/streptomycin were purchased from Gibco., fetal bovine serum (FBS) and 3-(4,5-dimethylthiazol-2-yl)-2,5-diphenyltetrazolium bromide (MTT) came from Biowest and Sigma, respectively.

2.2. Synthesis

2.2.1. Synthesis of Triiodoaniline

Firstly, 3 g aniline (30 mmol) and molecular 8.17 g iodine (60 mmol) were mixed in a 250 mL single neck round bottom flask. Then, hydrogen peroxide 30% (m = v) (60 - 120 mmol) was added to this mixture. The reaction mixture was sonicated at room temperature for 2 - 2.5 h, and the progress of the reaction was monitored by thin-layer chromatography (TLC) (11). Afterward, a saturated sodium thiosulfate aqueous solution (150 mL) was added to the mixture, which was extracted with dichloromethane (DCM, 50 mL $\times$ 5). The organic phase was dried over magnesium sulfate. After filtration, the solvent was concentrated by using an evaporator at 60°C to nearly 70 mL without reduced pressure. The solvent in 70 mL DCM was filtered fastly by column chromatography on silica gel by using DCM. Fractions containing the substance were combined after the column chromatography, and then the solvent was concentrated to nearly 50 mL at 60°C by using an evaporator (without reducing the pressure). When the solvent was left a little, triiodoaniline was crystallized in DCM for about three hours. After filtration, 2,4,6-triiodoaniline was obtained in a 91% yield, as shown in Figure 1.

2.2.2. Synthesis of the New Benzamide Derivative

The microwave irradiation method was used for 4N-TIB (12). A mixture of triiodoaniline (1eq) and 4-nitrobenzoyl chloride (1eq) in dioxane as solvent was reacted under microwave irradiation at 110°C for 10 min. The obtained solid raw product was filtered and washed with water and

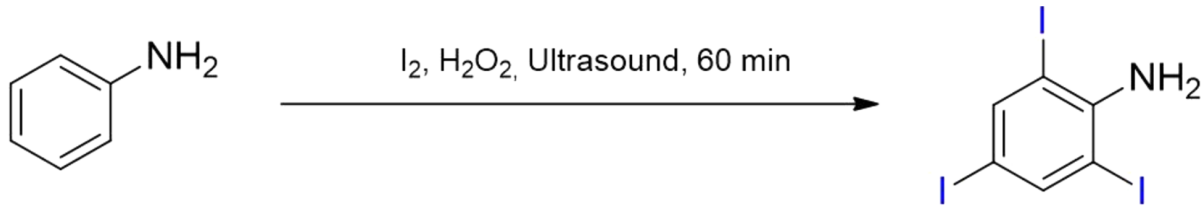

Figure 1. Synthesis of triiodoaniline

ethanol. 4N-TIB was obtained in an 85% yield, shown in Figure 2.

2.3. Characterization of 4N-TIB

The 1H and 13C nuclear magnetic resonance (NMR) spectra were recorded using tetramethylsilane (TMS) as the internal standard on a Varian Mercury 400MHz spectrometer using CDCl3 as the solvent. Coupling constants were given in hertz (Hz). Mass spectra (Q-TOF LC-MS) were recorded on "Agilent 6530 Accurate-Mass". The melting point (Mp) was obtained from the compound on the Electrothermal 9100 apparatus.

2.4. Drug Design and Characterization

2.4.1. Preparation of 4N-TIB Nanosuspension

The nanoprecipitation method was used in the preparation of nanosuspension based on the newly synthesized 4N-TIB (13, 14). For this purpose, 100 mg of 4N-TIB was weighed and dissolved in 1.25 mL DMSO for 10 min at 750 rpm in a magnetic stirrer. Later, 500 μL of Tween 60 was added and again mixed for 10 min. This organic phase was added drop by drop to the freshly prepared aqueous phase containing 0.5% PVA. At this stage, nanosuspension was obtained, and it was centrifuged at 10.000 rpm for 30 min. After the supernatant removal, the nanocrystals were washed several times with ultrapure water, and for the removal of DMSO residues, it was centrifuged again. Finally, the collapsed nanocrystals were resuspended by adding ultrapure water, frozen at -20°C, and subsequently lyophilized for 24 h. The obtained lyophilized nanosuspension was stored in a desiccator at room temperature to be used in experiments.

2.4.2. Yield, Particle Size, Zeta Potential Analysis, and Physical Stability of 4N-TIB Nanosuspension

Freshly prepared nanosuspension was used to perform this measurement. The particle size and distribution data, Polydispersity Index (PDI), and zeta potential values were determined by using the "Malvern Zetasizer Nano ZSP". One-hundred microliters of the nanosuspension formulation was measured at room temperature by diluting it in 900 μL of distilled water (n = 6). For long-term physical stability of 4N-TIB nanosuspension was evaluated after 12 (s of storage at room temperature. Particle size and distribution, PDI, and zeta potential values of the samples were measured using the same procedure explained above (n = 3). In addition, the yield of 4N-TIB nanosuspensions was calculated that freshly prepared and kept for 12 months (n = 3).

2.4.3. Viscosity of 4N-TIB Nanosuspensions

The viscosity of the 4N-TIB nanosuspensions, iohexol, and iopromide were measured using a capillary viscosimeter (Ubbelohde Capillary Viscosimeter, SI Analytics GmbH, Germany) at 20°C (15).

2.4.4. Investigation of the Surface Properties of 4N-TIB Nanosuspension

The 4N-TIB nanosuspension was examined morphologically with the help of scanning electron microscopy (SEM). For this purpose, lyophilized nanosuspension in powder form was analyzed by using the "Zeiss Sigma 300 SEM". Being non-conductive, the nanosuspensions were coated with approximately 100Å gold before the examination.

2.5. FT-IR Analysis of 4N-TIB Nanosuspension

The analysis was performed to examine whether a change had occurred in the contrast agent structure due to its reduction to the nanoscale and the interactions of formulation excipients with the contrast agent (16). Infrared spectra were carried out directly on the powder sample with the FT-IR spectrophotometer (Shimadzu IR Spirit-T) in the wavelength range of 4000 - 400 cm^{-1}.

2.6. CT Imaging

In order to determine the in-vitro density and contrast properties of the 4N-TIB nanosuspension, it was weighed to ensure that it contained 300 mg of iodine at the same

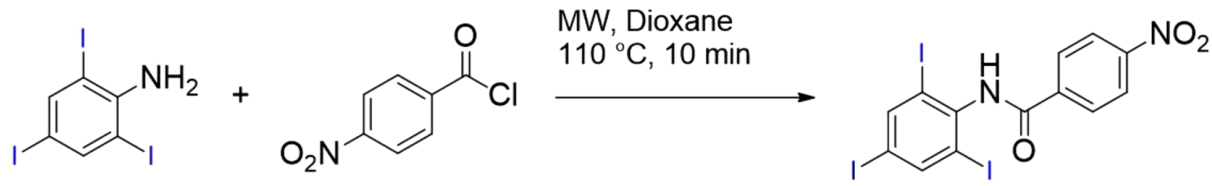

Figure 2. Synthesis of 4N-TIB

dose as the commercial contrast agents (iohexol and iopromide), and measurements were carried out in 1 mL of distilled water (n = 5). Samples (4N-TIB nanosuspension, iohexol and iopromide) were prepared in five different concentrations (5 mg iodine/mL, 25 mg iodine/mL, 75 mg iodine/mL, 150 mg iodine/mL and 300 mg iodine/mL). Afterward, the samples were placed in the CT gantry, and imaging was performed, as stated in Figure 3. Following that, the samples were placed in a water medium (to mimic the soft tissue environment), and CT imaging was performed again, as stated in Figure 4.

CT examinations were performed on a 320-row detector CT (Aquillion ONE Vision; Toshiba Medical Systems Corporation, Otawara, Japan) and a 256-row detector CT (Somatom® Definition Flash, Siemens Healthcare, Forchheim, Germany). The CT acquisition protocols were also followed under the different parameters depending on CT limits. CT scanners are described in Table 1.

Levene's statistics were used for the homogeneity analysis of group variances. The independent-samples *t*-test was conducted to determine the differences between 4N-TIB nanosuspension to iohexol and iopromide overall and each parameter, the significance level was accepted as $P < 0.05$ (17, 18).

2.7. Cell Culture

All cell culture experiments were performed at East Anatolian High Technology Research and Application Center (DAYTAM) of Ataturk University. Human embryonic kidney (HEK293T-ATCC® CRL-3216™) cells were used to evaluate the nephrotoxic effects of the 4N-TIB nanosuspension vis-a-vis commercially available radiocontrast iohexol and iopromide. The cells were cultured in Dulbecco's modified Eagle's medium (DMEM) supplemented with 10% fetal bovine serum (FBS) and 1% antibiotic solution of penicillin/streptomycin at 37°C in a humidified incubator with 5% CO_2. They were grown in T-25 culture flasks until they reached 70 - 80% confluence.

2.8. Cell Viability Assay

In order to evaluate the cellular toxicity of iohexol, iopromide, and 4N-TIB nanosuspension on kidney cells, an MTT assay was performed. Cells were seeded on a 96-well plate at 10.000 cells/well using a cell culture growth medium. The plate was incubated at 37°C and 5% CO_2 for 24 h to allow the cells to become adherent. Then, the cells were divided into nine groups. These groups were: negative control group, the radiocontrast agents (4N-TIB nanosuspension, iohexol, and iopromide) treated groups, and the positive control group. The negative control group was incubated with only a growth medium, whereas the positive control group was incubated in a cell culture medium including 300 μM H_2O_2 solution. The iodine concentration was calculated based on the iodine contents of each agent (iohexol 46.6% iodine; iopromide 48.12% iodine and 4N-TIB: 61.5% iodine). Radiocontrast agents containing the same amount of iodine (0.078 - 5 mg iodine/mL) were added to the treated groups. After 24 h, cells were observed under an inverted phase-contrast microscope (Zeiss Primovert Inverted Microscope, New York, USA). Then, 100 μL of 1 mg/mL MTT solution diluted in a serum-free medium was added to each well and mixed. After 4 h of incubation, the MTT solution was carefully removed from the wells. One-hundred-fifty microliters of DMSO was added to each well to dissolve the formazan crystals, and the plates were mixed thoroughly. The absorbance of the plate was read at 570 nm by using an Epoch Microplate Reader (BioTek Instruments). Each agent was assayed twice in sextuplicate. The cell viability was plotted as a percentage of the value obtained for negative control (19-21).

2.9. Statistical Analysis

One-way ANOVA followed by Dunnett's test was performed to calculate the significance of cellular viability results compared to negative control cells (GraphPad Software, Version 6.01). Data were shown as mean ± standard error of the mean. The significance levels were demonstrated as * $P < 0.05$, ** $P < 0.01$, *** $P < 0.001$, and **** $P < 0.0001$. Also, all other measurements and analyses were given as arithmetic mean and standard deviation.

Figure 3. The samples (upper line 4N-TIB nanosuspension, middle line iohexol, bottom line iopromide) are in the gantry of CT.

Table 1. Examination Parameters of Two Different CT Scanners

Variables	Somatom® Definition Flash (kVp)					Aquillion ONE Vision (kVp)			
	70	80	100	120	140	80	100	120	135
5 mAs	X	X	X	X	X	√	√	√	√
10 mAs	X	X	X	X	X	√	√	√	√
20 mAs	X	√	√	√	√	√	√	√	√
50 mAs	√	√	√	√	√	√	√	√	√
100 mAs	√	√	√	√	√	√	√	√	√
200 mAs	√	√	√	√	√	√	√	√	√

Abbreviations: CT, computed tomography; kVP, peak kilovolt; mAs, milliamper per second; X, cannot be performed; √, performed.

Figure 4. The samples (4N-TIB nanosuspension at the front, iohexol in the middle, and iopromide at the back) are in a water medium of CT.

3. Results

3.1. Characterization of 4N-TIB

NMR, Q-TOF and Mp results for 4N-TIB were as follows: (1) 4-nitro-N-(2,4,6-triiodophenyl) benzamide: solid, white, MP: 300 - 302°C; (2) 1H-NMR (400 MHz,d6-DMSO) δ (ppm): 8.19 (d, 2H, J:8.9, Ar-H), 8.26 (s, 2H, Ar-H), 8.39 (d, 2H, J:8.8, Ar-H), 10.75 (s, H, NHCO), 13C-NMR (100 MHz,d6-DMSO) δ (ppm): 96 (CAr-I), 102.96 (2xCAr-I), 124.54 (2xCHAr), 129.76 (2xCHAr), 140.04 (CAr), 142.18 (CAr), 146.80 (2xCHAr), 150.19 (CAr), 163.99 (C = O); (3) HRMS (Q-TOF) m/z calculated [M + H] + 620.75907, found [M + H] + 620.76871.

3.2. Drug Design and Characterization

3.2.1. Preparation of 4N-TIB Nanosuspension

The 4N-TIB nanosuspension was successfully prepared by using the nanoprecipitation method, and it showed a uniform and cube-like morphology. Optical microscope images of freshly prepared 4N-TIB nanosuspension are given in Figure 5.

3.2.2. Yield, Particle Size, Zeta Potential Analysis, and Physical Stability of 4N-TIB Nanosuspension

The yield, particle size, PDI, and zeta potential results of 4N-TIB nanosuspension, both fresh and 12 months old, are given in Table 2 as the mean and standard deviation. Additionally, size and zeta potential distribution graphs are shown in Figure 6.

3.2.3. Viscosity of 4N-TIB Nanosuspensions

Viscosity measurements of 4N-TIB nanosuspensions and contrast agents are given in Table 3.

3.2.4. Investigation of the Surface Properties of 4N-TIB Nanosuspension

The SEM images of 4N-TIB nanosuspension are given in Figure 7. The homogeneity of the size and size distribution

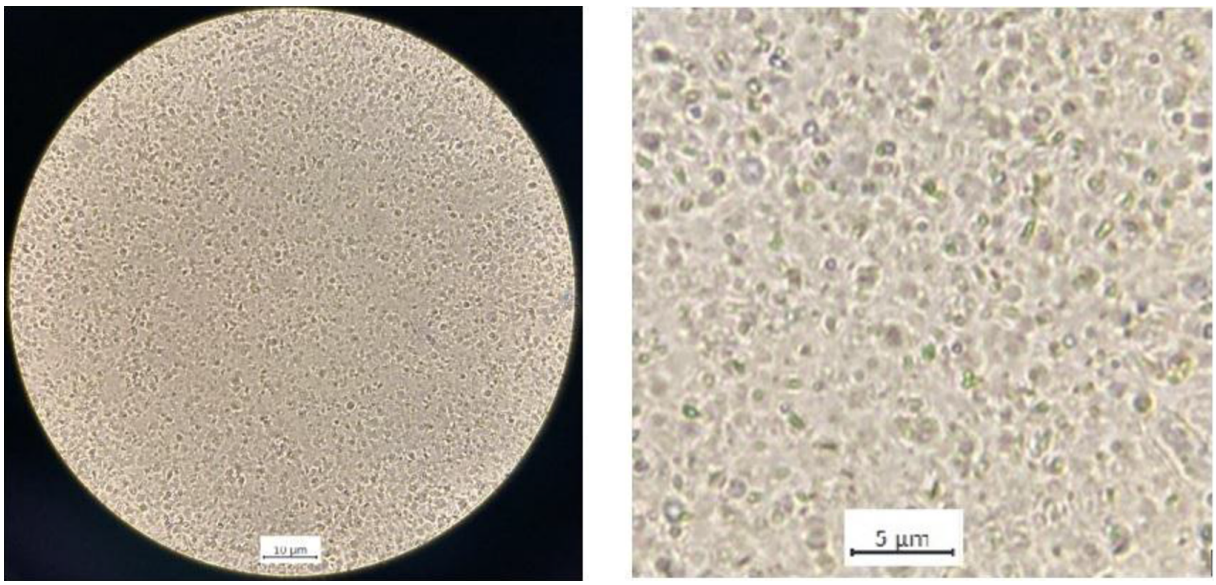

Figure 5. Optical microscope images of 4N-TIB nanosuspension

Table 2. Yield, Particle Size, PDI, and Zeta Potential Results of 4N-TIB Nanosuspensions

Variables	Particle Size (nm)	PDI	Zeta Potential (mV)	4N-TIB Nanosuspension Yield (%)
Freshly prepared	405.4 ± 5.96	0.168 ± 0.009	-14.8 ± 0.869	92.1 ± 3.25
After 12 months	412.3 ± 9.63	0.189 ± 0.012	-15.4 ± 0.211	91.8 ± 4.42

Table 3. Viscosity of 4N-TIB Nanosuspensions and Contrast Agents

Variable	Viscosity (cp)						
	Iohexol (300 mg/mL)	Iopromide (370 mg/mL)	4N-TIB (5 mg/mL)	4N-TIB (25 mg/mL)	4N-TIB (75 mg/mL)	4N-TIB (150 mg/mL)	4N-TIB (300 mg/mL)
20 (°C)	11.6	22.0	8.37	8.88	9.74	12.6	21.2

coincides with the results obtained through the zetasizer.

3.3. FT-IR Analysis of 4N-TIB Nanosuspension

The study was conducted to examine the interactions of the excipients in the formulation. The spectra of the newly synthesized 4N-TIB and 4N-TIB nanosuspension are given in Figure 8. The IR spectrum of the synthesized 4N-TIB molecule was examined, and the N-H bond was found to be around 3000-3500 cm-1, the C = O bond was around 1652.49 cm-1, the N = O band tension was around 1363 - 1286 cm^{-1}, and 2, 4, 6 tri-substituted benzene was around 800 - 850 cm^{-1}.

3.4. CT Imaging

All examinations were performed without problem. The axial CT image of 4N-TIB nanosuspension (upper line), iohexol (middle line), and iopromide (bottom line) was obtained. Five different concentrations (5 mg iodine/mL, 25 mg iodine/mL, 75 mg iodine/mL, 150 mg iodine/mL and 300 mg iodine/mL) of each sample were placed from left to right, respectively. The ROI measurements were performed for each sample, as shown in Figure 9. The HU values are also shown in this figure.

The mean density of the 4N-TIB nanosuspension was statistically and significantly higher than iohexol and iopromide ($P < 0.001$ for all). The mean densities of the 4N-TIB nanosuspension, iohexol, and iopromide were found at 1790.64 ± 800.80 HU, 1254.18 ± 719.68 HU, and 1091.89 ± 607.15, respectively for somatom. The mean density of the 4N-TIB nanosuspension was higher than those of iohexol and iopromide in all CT examinations. These findings were statistically significant for all parameters except 140 kVp, as given in Table 4.

A total of 86 CT examinations were performed for 15

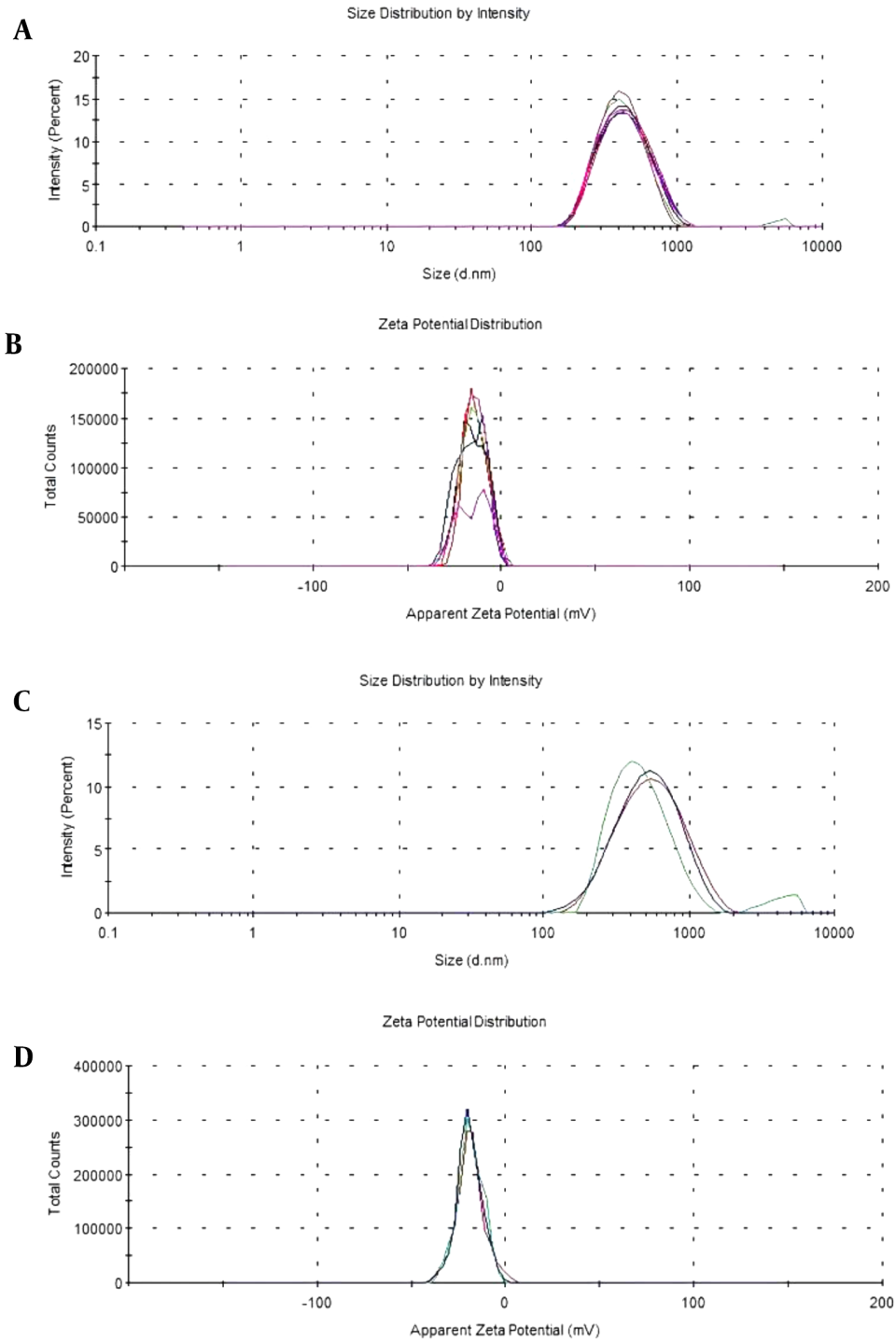

Figure 6. The size and zeta potential distribution of 4N-TIB nanosuspensions. A and B, are for fresh; C and D, are for 12 months old nanosuspensions.

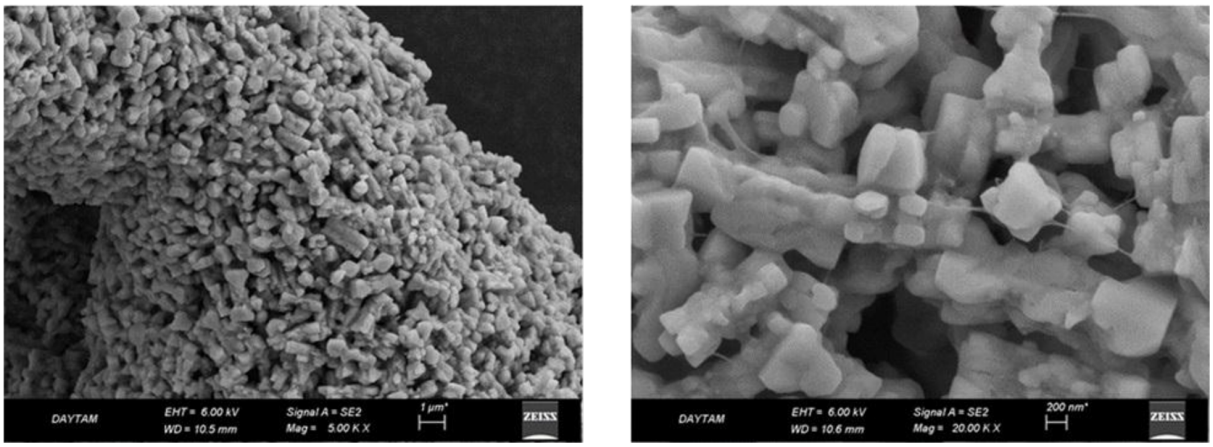

Figure 7. SEM images of 4N-TIB nanosuspension

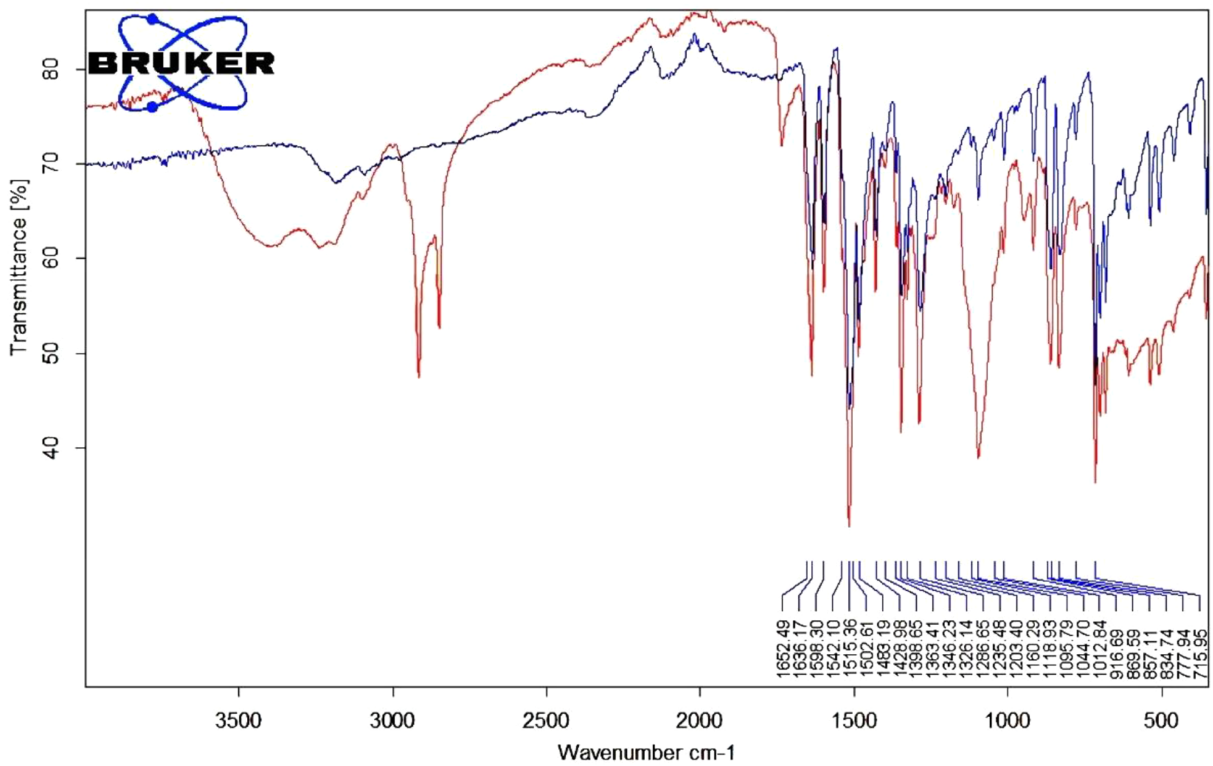

Figure 8. FT-IR spectra of newly synthesized pure 4N-TIB (blue) and 4N-TIB nanosuspension (red).

different samples. Twelve parameters were the same, and 19 parameters were different in two different machines because of their technical limitations. All the examinations were evaluated independently by one radiologist with seven (BP) years of experience in diagnostic radiology, who was blinded to all sample data on a 3D workstation (SyngoVia VB10B, Siemens Healthcare, Forchheim, Germany). A region of interest (ROI) was placed at the center of each sample. This process was repeated three times, and the mean value was recorded. All density data were

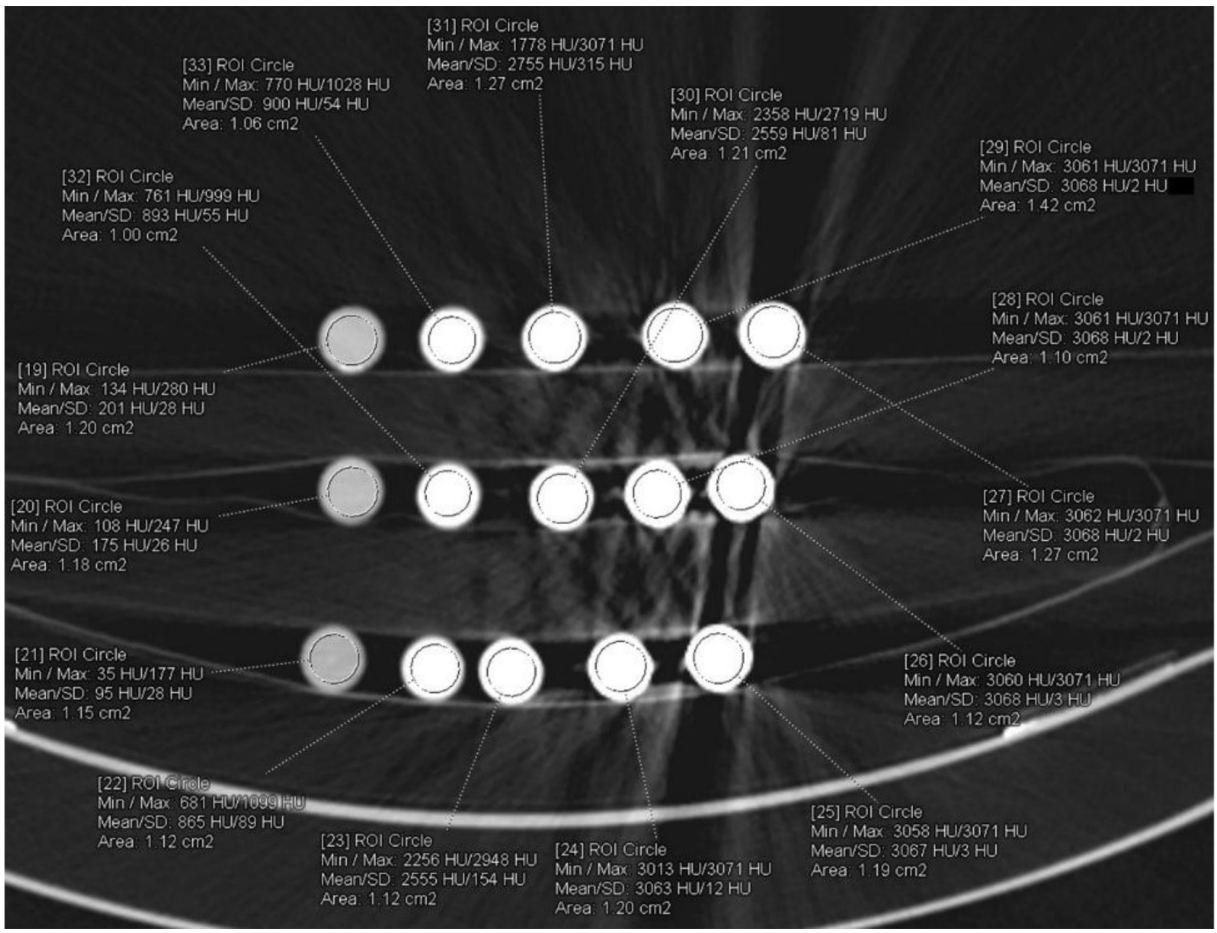

Figure 9. The axial CT (Somatom Definition Flash; 80 kVp, 100 mAs) image of 4N-TIB nanosuspension (upper line), iohexol (middle line), and iopromide (bottom line).

recorded from A1 to C5 according to the sample position in the image. The ROI was placed at the center of each sample for contrast analysis. This process was repeated three times, and the mean value was recorded (Figure 10). Another region of interest (ROI) was placed in the water near each sample (Figure 11).

The contrast value is calculated as HU value of sample -HU value of water. The axial CT image of 4N-TIB nanosuspension (right column), iohexol (middle column), and iopromide (left column) was also obtained. Five different concentrations (5 mg iodine/mL, 25 mg iodine/mL, 75 mg iodine/mL, 150 mg iodine/mL and 300 mg iodine/mL) of each sample were placed from top to bottom, respectively. The ROI measurements were performed for each sample and the adjacent water, as seen in Figures 10 and 11.

The mean contrast value of the 4N-TIB nanosuspension was statistically and significantly higher than those of iohexol and iopromide ($P < 0.001$ for all). The mean contrast values of 4N-TIB nanosuspension, iohexol, and iopromide were 1800.36 $\pm$ 810.13 HU, 1276.32 $\pm$ 732.14 HU, and 1098.92 $\pm$ 611.36, respectively, for somatom. The mean contrast value of the 4N-TIB nanosuspension was higher than those of iohexol and iopromide in all CT examinations. These findings were statistically significant for all parameters except 140 kVp, as given in Table 5.

3.5. Cell Viability Assay

Cellular toxicity of the 4N-TIB nanosuspension was determined by performing an MTT analysis with respect to the commercially available radiocontrast agents (iohexol and iopromide). Cell viability results of iohexol, iopromide, and the 4N-TIB nanosuspension are shown in Figure 12. No significant differences in cell viability were obtained for the low doses of studied radiocontrast agents and 4N-TIB nanosuspension. However, significant decreases were found at high concentrations (1.25 - 5 mg Iodine/mL). Five

Table 4. The Mean Density Values of Different CT Scanners and CT Parameters

Variables	4N-TIB Nanosuspension (HU)	Iohexol (HU)	Iopromide (HU)	P-Values
Overall	1790.64 ± 800.80	1254.18 ± 719.68	1091.89 ± 607.15	< 0.001 for all
Somatom®	1750.04 ± 950.72	1261.5 ± 692.58	1041.2 ± 439.14	< 0.001 for all
Aqulion ONE	1824.04 ± 655.94	1248.18 ± 744.21	1133.36 ± 715.32	< 0.001 for all
70 kVp [a]	2119.47 ± 948.8	1470.93 ± 658.49	1207.33 ± 61.43	0.039; 0.002
80 kVp	2162.8 ± 1053.72	1627.83 ± 1183.27	1428.11 ± 1127.42	0.05; 0.006
100 kVp	1818.24 ± 643.04	1160.46 ± 369.59	1003.72 ± 168.36	0.001 for all
120 kVp	1679.54 ± 734.61	1126.68 ± 568.2	955.5 ± 394.55	0.001 for all
135 kVp [a]	1594 ± 425.16	1024 ± 352	937.03 ± 255.51	0.001 for all
140 kVp [b]	1397.45 ± 856.44	1136 ± 880.23	1010.6 ± 817.62	0.061; 0.056
5 mAs	1646.93 ± 247.1	1063.93 ± 257.86	993 ± 226.37	0.001 for all
10 mAs	1718.87 ± 407.01	1136.2 ± 372.89	1011.4 ± 254.22	0.001 for all
20 mAs	1741.69 ± 760.12	1136.17 ± 501.62	981 ± 379.66	0.001 for all
50 mAs	1882.04 ± 1076.74	1412.8 ± 1116.26	1293.11 ± 1088.64	0.045; 0.012
100 mAs	1813.13 ± 795.85	1279.8 ± 635.55	1092.04 ± 439.82	0.001; < 0.001
200 mAs	1787.09 ± 754.44	1264.44 ± 614.84	1036.56 ± 283.74	0.001; < 0.001

[a] These parameters were only found in Aqulion.
[b] This parameter was only found in Somatom.

Table 5. The Mean Contrast Values of Different CT Scanners and CT Parameters

Variables	4N-TIB Nanosuspension (HU)	Iohexol (HU)	Iopromide (HU)	P-Values
Overall	1800.36 ± 810.13	1276.32 ± 732.14	1098.92 ± 611.36	< 0.001 for all
Somatom®	1741.47 ± 965.66	1282.73 ± 700.08	1046.87 ± 455.36	< 0.001 for all
Aqulion ONE	1846.98 ± 672.02	1271.24 ± 752.68	1140.12 ± 726.84	< 0.001 for all
70 kVp [a]	2185.45 ± 952.2	1484.22 ± 666.54	1222.24 ± 654.2	0.036; 0.002
80 kVp	2164.72 ± 1065.8	1636.62 ± 1195.4	1441.34 ± 1141.68	0.047; 0.005
100 kVp	1832.36 ± 651.2	1173.81 ± 382.42	1024.82 ± 171.54	< 0.001 for all
120 kVp	1693.85 ± 734.58	1141.64 ± 574.42	971.64 ± 398.64	< 0.001 for all
135 kVp [a]	1602.02 ± 424.85	1036.24 ± 358.6	953.08 ± 256.8	< 0.001 for all
140 kVp [b]	1403.15 ± 863.2	1185.12 ± 896.58	1021.48 ± 826.71	0.059; 0.053
5 mAs	1667.87 ± 252.21	1084.1 ± 261.5	1005.24 ± 231.21	< 0.001 for all
10 mAs	1733.37 ± 406.02	1146.63 ± 384.21	1032.69 ± 260.04	< 0.001 for all
20 mAs	1752.87 ± 765.2	1150.86 ± 510.8	1000.24 ± 381.54	< 0.001 for all
50 mAs	1896.56 ± 1084.54	1432.4 ± 1126.54	1313.3 ± 1096.98	0.042; 0.011
100 mAs	1898.33 ± 805.52	1304.62 ± 642.2	1102.26 ± 443.82	0.001; < 0.001
200 mAs	1903.21 ± 632.54	1302.52 ± 621.5	1040.16 ± 288.51	0.001; < 0.001

[a] These parameters were only found in Aqulion.
[b] This parameter was only found in Somatom.

miligrams Iodine/mL concentration for both iohexol and iopromide significantly reduced cellular viability by 30% vis a vis negative control. However, this decrease was found to be 20% in the 4N-TIB nanosuspension group.

4. Discussion

The preparation of formulations of active substances with water-insolubility is a critical problem to be overcome in drug design. There are many ways to solve this problem

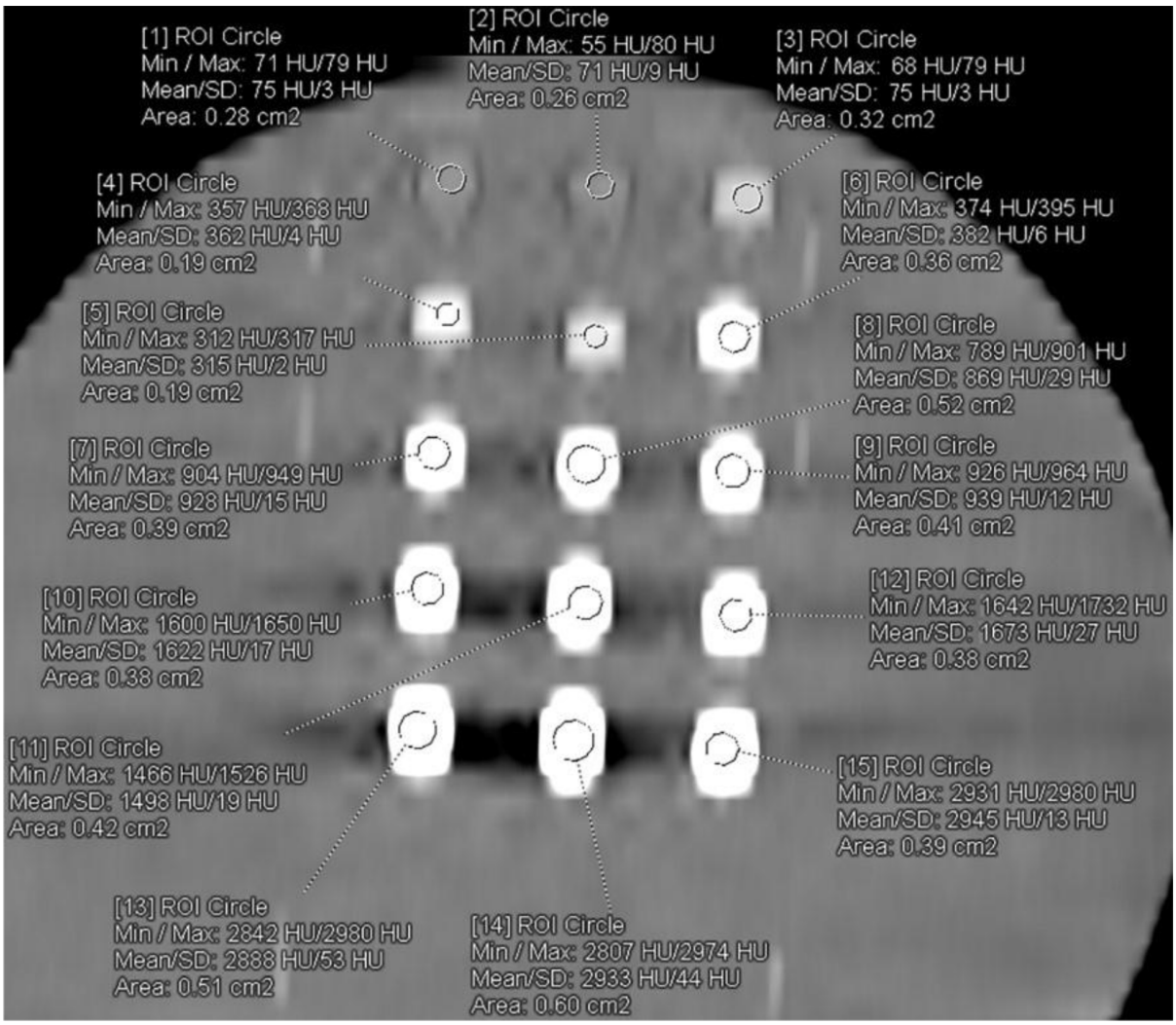

Figure 10. The axial CT (Aquilion One Vision; 70 kVp, 200 mAs) image of 4N-TIB nanosuspension (right column), iohexol (middle column), and iopromide (left column) in water medium. The ROIs were placed at the center of each sample.

of active substances and increase their bioavailability, such as the use of surfactants, inclusion complexing, use of co-solvent, and preparation of solid dispersions. In particular, reducing particle size to nanosize is one of the ways developed to solve this problem (22, 23). The rate of dissolution, permeation, and bioavailability increases with reduction in size and increase in surface area; the administered dose, side effects, and toxicity, together with drug consumption and cost, are also reduced (24).

With this aim in view, an iodine-containing contrast agent (4N-TIB) was synthesized from triiodoaniline. The advantages of this method are that it enables working in an aqueous medium, shortens the reaction time, and increases the yield (7). In the study, triiodoaniline synthesis was performed by applying the procedure recorded in the literature. However, in our study, we worked at 10 times the scale and made minor modifications to the workup processes after the synthesis. In the literature, the mixture is extracted with ethyl acetate after adding saturated sodium thiosulfate aqueous solution, but the mixture was extracted with DCM in our study. The procedure of column chromatography has not been explained in detail in the literature (11). In this study, the column chromatography and the workup procedures after it are explained in detail. Too much solvent is consumed in the workup processes, but it poses no problem since only DCM (with a low boiling point) is used as the solvent, and it can easily be reused by distillation. In the literature, N-(4-iodophenyl) benza-

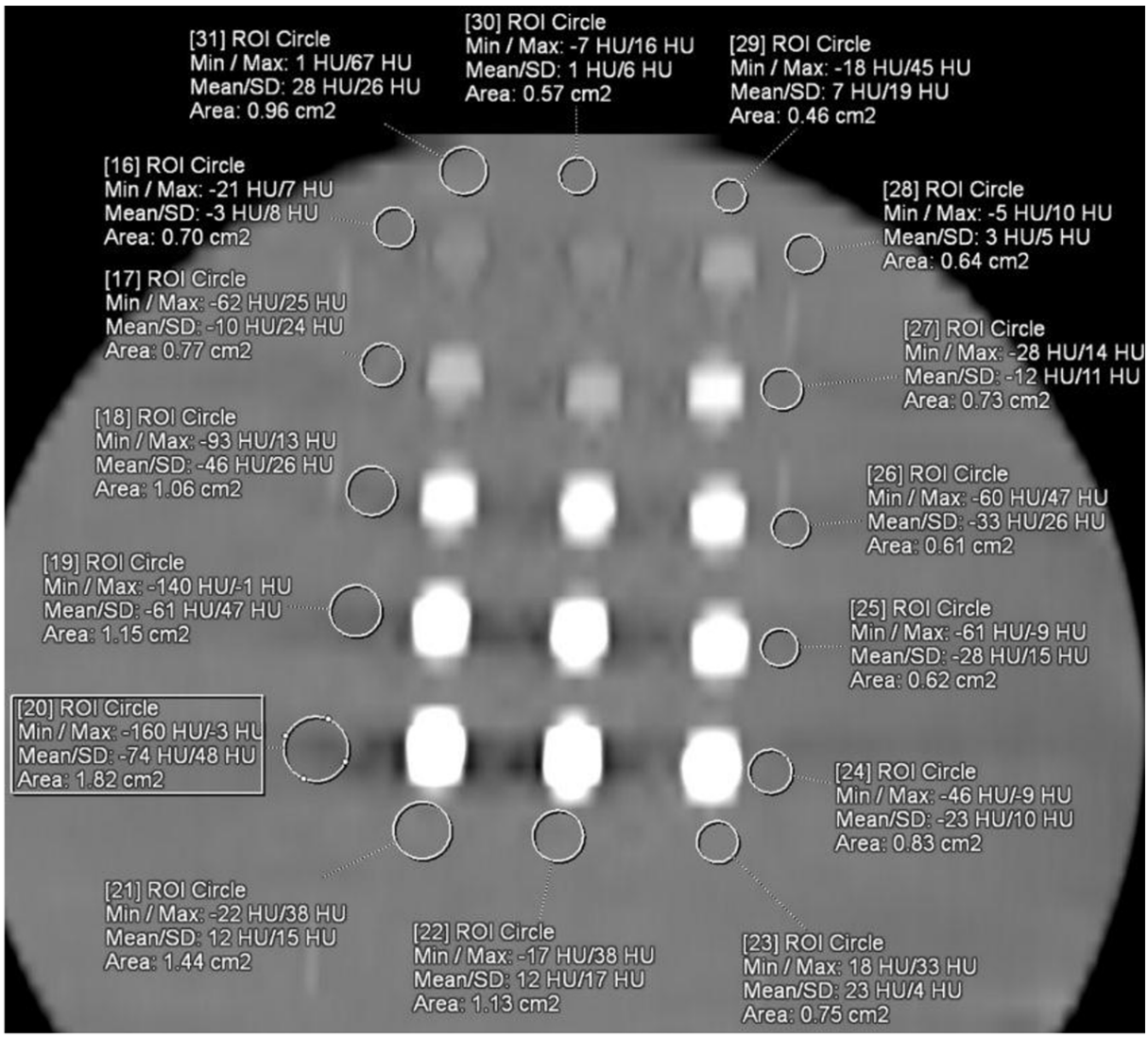

Figure 11. It shows the axial CT (Aquilion One Vision; 70 kVp, 200 mAs) image of 4N-TIB nanosuspension (right column), iohexol (middle column), and iopromide (left column) in water medium. The ROIs are seen placed next to the samples.

mide is synthesized at room temperature with 86% yield in 12 hours (25). In our research, 4N-TIB was synthesized under microwave irradiation with high efficiency (85%) in 10 minutes, which had three times the iodine content of N-(4-iodophenyl) benzamide. Microwave irradiation and ultrasound-promoted synthesis are important in shortening the reaction time and increasing the product yield for green chemistry (26). In order to obtain a more stable high yield product in the synthesis, benzoyl chloride carrying an electron-withdrawing nitro group in the 4th position was preferred. In addition, it was aimed to have the long-term stability of this synthesized contrast.

The insolubility of the synthesized 4N-TIB molecule in water provided nanosuspensions. Due to the high content of iodine in the preparation, the contrast properties were evaluated. In this context, contrast properties were compared with other iodine-containing preparations currently used in CT imaging. Our goal was to investigate whether it was possible to obtain similar contrast properties from existing contrast agents by using fewer chemicals.

Available contrast agents are rapidly excreted via the kidneys after administration and allow only a short imaging time. In addition, these agents disperse non-

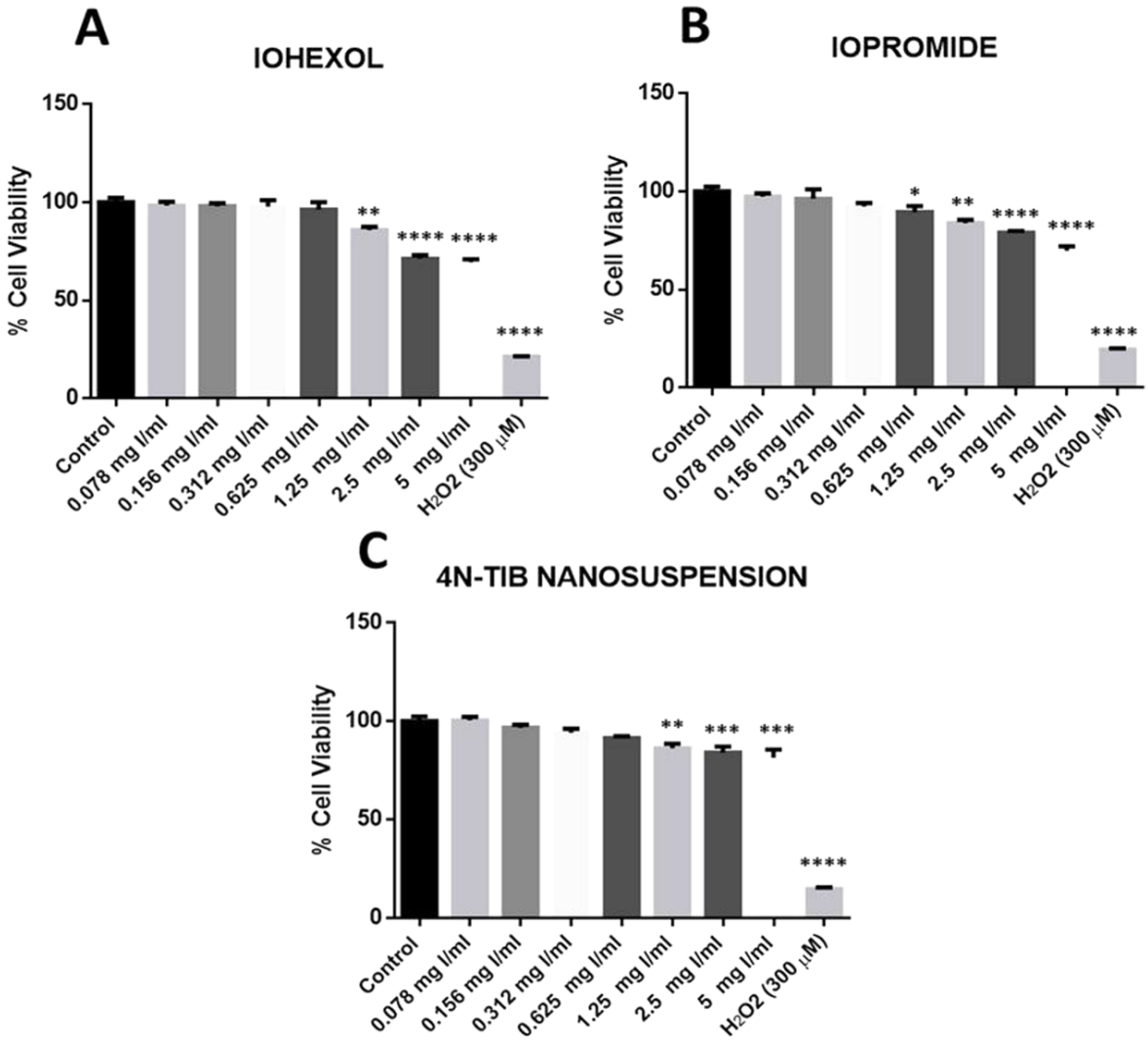

Figure 12. Effect of iohexol, iopromide, and 4N-TIB nanosuspension on the cell viability of HEK-293T cells. Cell viability was determined using an MTT assay and expressed as a percentage of the negative control cells. The cell viability (%) is expressed as the mean ± standard error of the mean of two independent measurements (asterisks indicate * $P < 0.05$, ** $P < 0.01$, *** $P < 0.001$, and **** $P < 0.0001$).

specifically into the intravascular and extravascular spaces resulting in unclear CT images. The nanosized contrast agents have been developed to overcome these limitations (27).

It is exciting that the physical properties of nanomaterials differ significantly from those of bulk materials with the same chemical compositions. The physical properties of nanomaterials are highly dependent on the size and morphology of the nanoparticles. These differences include melting point, change in cellular uptake parameters, change in magnetic and optical properties, the conductivity of the material, etc. When we compare bulk materials and nanomaterials in terms of surface-to-volume ratio, it has been seen that this ratio has a significant effect on the occurrence of new physical properties. As the particle size decreases, the number of atoms on the surface (compared to the total atomic number) increases. As the particles get smaller, the surface/volume ratio increases and the effect of the structure on the magnetic properties becomes greater (28).

Also, nanosized particles have unique properties. Especially the rate of dissolution, permeation, and bioavailability increases with reduction in size and increase in the surface area; the administered dose, side effects, toxicity,

and therefore drug consumption and cost are also reduced (24). Nanosuspensions can be administered by oral, parenteral, dermal, ocular, and pulmonary routes and can be targeted to the desired tissue (29). It has been reported that the circulation half-life of nanoparticles is up to 15h whereas that of iodine molecules is only minutes. In addition, nanoparticles can be multifunctional, and they provide contrast or therapeutic effects for multiple imaging methods such as CT, MRI, and fluorescence. Nanoparticles may be compatible with patients for whom conventional iodinated contrast agents are contraindicated due to renal failure or allergic responses (9). These particles increase the transport efficiency of drugs and reduce the side effects of free drugs, such as non-specific distribution, owing to their long circulation time and targeting capabilities (30). The literature is replete with imaging studies that have been conducted by reducing many iodine-based contrast agents to nanosize (9). Today, studies are carried out using many nanoparticular contrast agents in X-ray imaging (especially of heart, vessel, lung, bone, spleen, and liver) (31). In addition, nanoparticular contrast agent studies (350 - 400 nm) on the kidneys are also available in the literature (10). Imaging studies with iodine-containing nanoparticular drugs are also increasing in the literature (2, 32). In our study, it was found that the presence of iodine was much denser in the 4N-TIB nanosuspension than in the contrasting agents, iohexol and iopromide when the volumes of all the three materials used were uniform. The study consisted of 86 CT examinations that were performed with a total of 31 different parameters in two different devices. This result shows that 4N-TIB nanosuspensions will produce similar contrast with less iodine. This is especially important in contrast to nephropathy, which develops due to the reaction of the kidneys to contrast imaging and sometimes requires dialysis. This is because the risk of developing contrast nephropathy increases as the amount of contrast material increases (33). This study obtained similar contrast properties with less iodine content by using nanoscale iodine contrast material. We speculate that nanosuspensions may be helpful in preventing contrast nephropathy. However, this needs to be confirmed by more specific studies.

The nanoprecipitation method is commonly used to prepare nanosuspensions as a drug delivery system. The nanosuspension technology is an excellent formulation approach for poorly water-soluble drugs. This method requires minimum equipment and excipients, and therefore it is economical (34). For 4N-TIB, DMSO is an excellent solvent, and Tween 60 is a very useful non-ionic surfactant/stabilizer used in this study. During transition from the organic to the aqueous phase, the particles that did not form aggregates did so with the help of PVA which was used as a polymeric stabilizer. In nanosuspension formulations, stabilizers should interact effectively with the crystal surface to provide physical stability to the formulations by preventing their agglomeration via steric or ionic barriers. Non-ionic and polymeric stabilizers increase the physical stability of nanosuspension formulations by steric stabilization (35).

Particle size, size distribution, PDI, and zeta potential are essential characterization parameters for the physical stability of nanosuspensions. PDI indicates a degree of the particle size distribution for nanosuspensions. A higher value of PDI indicates broad particle distribution and a lower, narrow particle distribution (34). For a physically stable nanosuspension stabilized only by electrostatic repulsion, a minimum zeta potential of $\pm$ 30 mV is required. However, in electrostatic and steric stabilization, a zeta potential of $\pm$ 20 mV is sufficient (36). The results showed that the mean particle size, PDI, and the zeta potential values of the freshly prepared and the 12 months old nanosuspensions were 405.4 nm, 0.168, -14.8 mV, and 412.3 nm, 0.189, -15.4 mV, respectively. When the sizes of the freshly prepared and the 12 months old nanosuspensions and their PDI, as well as zeta potential values, were compared, all values showed a minimum increase, but this increase did not impair the physical stability of the nanosuspensions as the zeta potential of these particles supported it. In the studies, it has been stated that nanoparticles, especially those below $\pm$ 5 mV, have an aggregate forming potential (22, 37). A study by Abdelbary et al. examined the effects of different polymeric stabilizers on aripiprazole nanosuspensions. In their study, the high surface concentration of the stabilizer and the elongation of the hydrophilic chains in the aqueous phase were found to have increased the thickness of the polymer layer on the nanocrystal surface. This situation increased the zeta potential value. It was emphasized that despite the increase in the size of the nanoparticles, the stability continued with the increasing zeta potential, and the steric stabilization was positively affected by the zeta potential (38). When we look at the values after 12 months in our study, we can say that the same effect was observed, and this situation was positive in terms of stability. Ali et al, prepared hydrocortisone nanosuspensions and kept them at 25°C for 3 weeks to evaluate their physical stability. While the dimensions of fresh nanosuspensions were 500 nm, they reached 687 nm with an increase of 187 nm after 3 weeks. The zeta potential value of freshly prepared nanosuspensions was found to be -18 mV, and authors stated that nanosuspensions with these values remained stable (39). There was a minimum size increase of only 7 nm in 12 months in our study. The increase in the zeta potential and the PDI value hovering close to zero showed that the nanosuspensions

that we had prepared remained stable for a long time.

There are few studies on polymeric nano-contrast agents in the literature. As we did not use a polymeric system in our study, all of our iodine-containing active substance was converted into nanosuspensions. It provided us with an advantage in terms of efficiency. In a previous study, for example, iodine-containing nanoparticles were prepared with about 45% iodine, and this ratio proved to be quite disadvantageous for contrast imaging (27). In another study, although the stability of nanoparticles prepared with methacrylate polymer was suitable, they provided poor contrast due to 55% iodine content (40). In yet another study for contrast imaging, it was observed that polymeric particles were not useful in biomedical applications due to their 1 μm size (41). Our nanoparticles offered a very high iodine content as they had been prepared entirely from 4N-TIB, around 400 nm, and without polymers. In terms of stability, no significant change was observed even after 1 year of data collection.

Contrast media can cause direct toxic effects on kidney cells, thus damaging the kidney. The increased viscosity of the contrast agents compromises blood flow and oxygen supply to the critical region of the kidney, delaying tubular filtration and impairing glomerular filtration, possibly as a result of increased tubular fluid viscosity. Thus, using low-viscosity agents in contrast imaging is very important) (42, 43). In our study, the viscosities of 4N-TIB nanosuspensions were measured and evaluated together with those of iopromide and iohexol. The obtained results found that the viscosity value of 4N-TIB particles was lower than that of iopromide and iohexol, especially at low concentrations.

Our formulation consisted of 4N-TIB, DMSO, and PVA. DMSO was removed by washing with water several times during the nanosuspension preparation process. Thus, only PVA and 4N-TIB remained in the nanocrystal structure. The FT-IR spectrum showed two specific band groups. One band stretching from the nanosuspension spectrum on the left side was seen in the 3500-3200 cm-1, and it was different from the 4N-TIB spectrum. This band referred to PVA, and in the Mohyeldin et al. study, the characteristic band of PVA was seen at this band gap (35). The other band group on the right side of the nanosuspension spectrum was in harmony with 4N-TIB and there was even an overlap between the two. It demonstrated that 4N-TIB in the nanosuspension formulation had no interaction with PVA. Compared to the synthesized 4N-TIB, it was also shown that the 4N-TIB nanosuspension did not have any undesirable interaction and that it exhibited similarity with the synthesized molecule.

The HU values of contrast agents are affected by several factors such as contrast concentration, X-ray tube kVp, mAs, detector, and CT algorithms. We observed certain variability in the same contrast agent in our results. It was probably due to the fact that we used different parameters on two different devices (with different detectors and algorithms). Although these values varied within themselves, 4N-TIB nanosuspension had a statistically higher HU value than those of the other contrast agents in all parameters. In the first three doses as shown in Figure 9 (5 mg iodine/mL, 25 mg iodine/mL, 75 mg iodine/mL), it was observed that the 4N-TIB nanosuspension displayed much more contrast although it contained the same amount of iodine as iohexol and iopromide. In particular, the nanosuspension containing 75 mg Iodine/mL exhibited significantly more contrast properties in relation to the two commercial contrast agents currently in use.

Cell viability assay indicated that the 4N-TIB nanosuspension has a significantly less impact on cellular viability. Increased cell viability at the higher doses of contrast agents was also detected on the rat kidney epithelial cell line NRK 52-E by Jensen et al. (44). The toxic effects were increasingly observed especially in 24 h treatments. An increase in cellular toxicity mediated by iodine-containing contrast agents was also detected in previous studies on renal epithelial cells and CHO cells (45, 46). In the current study, the low cellular toxicity of the newly synthesized contrast agents at higher concentrations offers immense potential for use in imaging.

4.1. Conclusion

Nanoparticles are a useful platform in developing contrast agents for molecular imaging. They are small enough to penetrate most tissues and can be designed to be detected by standard radiological methods (47). In this study, the newly synthesized 4N-TIB can be used in CT imaging as it contains less iodine in its structure, but it is a water-insoluble contrast agent. In conclusion, it can be said that at low doses, 4N-TIB nanosuspensions show greater contrast properties in CT imaging than iopromide and iohexol do while containing a uniform amount of iodine. Also, in-vitro cellular viability findings indicate that the 4N-TIB nanosuspension has lower cytotoxicity than commercial radiocontrast agents. Thus, 4N-TIB nanosuspensions can be an alternative to existing iodine-containing contrast agents. However, all these studies need to be supported with more detailed experiments on laboratory animals.

Acknowledgments

Thanks to Atatürk University, which supported us in this study with its laboratory facilities.

Footnote

Conflict of Interests: The authors declare that there are no conflicts of interest.

References

1. Lusic H, Grinstaff MW. X-ray-computed tomography contrast agents. *Chem Rev*. 2013;**113**(3):1641–66. doi: 10.1021/cr200358s. [PubMed: 23210836]. [PubMed Central: PMC3878741].
2. Koc MM, Aslan N, Kao AP, Barber AH. Evaluation of X-ray tomography contrast agents: A review of production, protocols, and biological applications. *Microsc Res Tech*. 2019;**82**(6):812–48. doi: 10.1002/jemt.23225. [PubMed: 30786098].
3. Krause W. Iodinated X-Ray Contrast Agents. In: Kaiho T, editor. *Iodine Chemistry and Applications*. New Jersey, USA: John Wiley & Sons; 2014. p. 353–74. doi: 10.1002/9781118909911.ch19.
4. Caschera L, Lazzara A, Piergallini L, Ricci D, Tuscano B, Vanzulli A. Contrast agents in diagnostic imaging: Present and future. *Pharmacol Res*. 2016;**110**:65–75. doi: 10.1016/j.phrs.2016.04.023. [PubMed: 27168225].
5. Keaney JJ, Hannon CM, Murray PT. Contrast-induced acute kidney injury: how much contrast is safe? *Nephrol Dial Transplant*. 2013;**28**(6):1376–83. doi: 10.1093/ndt/gfs602. [PubMed: 23413087].
6. Han X, Xu K, Taratula O, Farsad K. Applications of nanoparticles in biomedical imaging. *Nanoscale*. 2019;**11**(3):799–819. doi: 10.1039/c8nr07769j. [PubMed: 30603750]. [PubMed Central: PMC8112886].
7. Ravichandran R. Nanoparticles in drug delivery: potential green nanobiomedicine applications. *Int J Green Nanotechnol Biomed*. 2009;**1**(2):B108–30.
8. Wang L, Du J, Zhou Y, Wang Y. Safety of nanosuspensions in drug delivery. *Nanomedicine*. 2017;**13**(2):455–69. doi: 10.1016/j.nano.2016.08.007. [PubMed: 27558350].
9. Cormode DP, Naha PC, Fayad ZA. Nanoparticle contrast agents for computed tomography: a focus on micelles. *Contrast Media Mol Imaging*. 2014;**9**(1):37–52. doi: 10.1002/cmmi.1551. [PubMed: 24470293]. [PubMed Central: PMC3905628].
10. Williams RM, Shah J, Tian HS, Chen X, Geissmann F, Jaimes EA, et al. Selective Nanoparticle Targeting of the Renal Tubules. *Hypertension*. 2018;**71**(1):87–94. doi: 10.1161/HYPERTENSIONAHA.117.09843. [PubMed: 29133360]. [PubMed Central: PMC5730475].
11. Ferreira IM, Casagrande GA, Pizzuti L, Raminelli C. Ultrasound-Promoted Rapid and Efficient Iodination of Aromatic and Heteroaromatic Compounds in the Presence of Iodine and Hydrogen Peroxide in Water. *Synth Commun*. 2014;**44**(14):2094–102. doi: 10.1080/00397911.2013.879900.
12. Yerdelen KO, Koca M, Anil B, Sevindik H, Kasap Z, Halici Z, et al. Synthesis of donepezil-based multifunctional agents for the treatment of Alzheimer's disease. *Bioorg Med Chem Lett*. 2015;**25**(23):5576–82. doi: 10.1016/j.bmcl.2015.10.051. [PubMed: 26514744].
13. Pandya VM, Patel JK, Patel DJ. Formulation, optimization and characterization of simvastatin nanosuspension prepared by nanoprecipitation technique. *Der Pharm Lett*. 2011;**3**(2):129–40.
14. Sahu BP, Das MK. Nanosuspension for enhancement of oral bioavailability of felodipine. *Appl Nanosci*. 2013;**4**(2):189–97. doi: 10.1007/s13204-012-0188-3.
15. Jost G, Pietsch H, Lengsfeld P, Hutter J, Sieber MA. The impact of the viscosity and osmolality of iodine contrast agents on renal elimination. *Invest Radiol*. 2010;**45**(5):255–61. doi: 10.1097/RLI.0b013e3181d4a036. [PubMed: 20375847].
16. Sevinc Ozakar R, Ozakar E. Current Overview of Oral Thin Films. *Turk J Pharm Sci*. 2021;**18**(1):111–21. doi: 10.4274/tjps.galenos.2020.76390. [PubMed: 33634686]. [PubMed Central: PMC7957312].
17. Pirimoglu B, Sade R, Sakat MS, Polat G, Kantarci M. Low-dose non-contrast examination of the temporal bone using volumetric 320-row computed tomography. *Acta Radiol*. 2019;**60**(7):908–16. doi: 10.1177/0284185118802597. [PubMed: 30249112].
18. Pirimoglu B, Sade R, Sakat MS, Ogul H, Levent A, Kantarci M. Low-Dose Noncontrast Examination of the Paranasal Sinuses Using Volumetric Computed Tomography. *J Comput Assist Tomogr*. 2018;**42**(3):482–6. doi: 10.1097/RCT.0000000000000699. [PubMed: 29287024].
19. Tolosa L, Donato MT, Gomez-Lechon MJ. General Cytotoxicity Assessment by Means of the MTT Assay. *Methods Mol Biol*. 2015;**1250**:333–48. doi: 10.1007/978-1-4939-2074-7_26. [PubMed: 26272156].
20. Kumar P, Nagarajan A, Uchil PD. Analysis of Cell Viability by the MTT Assay. *Cold Spring Harb Protoc*. 2018;**2018**(6). doi: 10.1101/pdb.prot095505. [PubMed: 29858338].
21. Rai Y, Pathak R, Kumari N, Sah DK, Pandey S, Kalra N, et al. Mitochondrial biogenesis and metabolic hyperactivation limits the application of MTT assay in the estimation of radiation induced growth inhibition. *Sci Rep*. 2018;**8**(1):1531. doi: 10.1038/s41598-018-19930-w. [PubMed: 29367754]. [PubMed Central: PMC5784148].
22. Afifi SA, Hassan MA, Abdelhameed AS, Elkhodairy KA. Nanosuspension: An Emerging Trend for Bioavailability Enhancement of Etodolac. *Int J Polym Sci*. 2015;**2015**:1–16. doi: 10.1155/2015/938594.
23. Pawar VK, Singh Y, Meher JG, Gupta S, Chourasia MK. Engineered nanocrystal technology: in-vivo fate, targeting and applications in drug delivery. *J Control Release*. 2014;**183**:51–66. doi: 10.1016/j.jconrel.2014.03.030. [PubMed: 24667572].
24. Verma S, Kumar S, Gokhale R, Burgess DJ. Physical stability of nanosuspensions: investigation of the role of stabilizers on Ostwald ripening. *Int J Pharm*. 2011;**406**(1-2):145–52. doi: 10.1016/j.ijpharm.2010.12.027. [PubMed: 21185926].
25. Hong J, Liu Q, Li F, Bai G, Liu G, Li M, et al. Electrochemical Radical Borylation of Aryl Iodides. *Chin J Chem*. 2019;**37**(4):347–51. doi: 10.1002/cjoc.201900001.
26. Nain S, Singh R, Ravichandran S. Importance of Microwave Heating In Organic Synthesis. *Advanced Journal of Chemistry-Section A*. 2019;**2**(2):94–104. doi: 10.29088/sami/ajca.2019.2.94104.
27. Lee N, Choi SH, Hyeon T. Nano-sized CT contrast agents. *Adv Mater*. 2013;**25**(19):2641–60. doi: 10.1002/adma.201300081. [PubMed: 23553799].
28. Čitaković N. Physical properties of nanomaterials. *Vojnoteh Glas*. 2019;**67**(1):159–71. doi: 10.5937/vojtehg67-18251.
29. Malkani A, Date AA, Hegde D. Celecoxib nanosuspension: single-step fabrication using a modified nanoprecipitation method and in vivo evaluation. *Drug Deliv Transl Res*. 2014;**4**(4):365–76. doi: 10.1007/s13346-014-0201-3. [PubMed: 25787068].
30. Kim J, Lee N, Hyeon T. Recent development of nanoparticles for molecular imaging. *Philos Trans A Math Phys Eng Sci*. 2017;**375**(2107). doi: 10.1098/rsta.2017.0022. [PubMed: 29038377]. [PubMed Central: PMC5647266].
31. Ashton JR, West JL, Badea CT. In vivo small animal micro-CT using nanoparticle contrast agents. *Front Pharmacol*. 2015;**6**:256. doi: 10.3389/fphar.2015.00256. [PubMed: 26581654]. [PubMed Central: PMC4631946].
32. Hainfeld JF, Ridwan SM, Stanishevskiy Y, Smilowitz NR, Davis J, Smilowitz HM. Small, Long Blood Half-Life Iodine Nanoparticle for Vascular and Tumor Imaging. *Sci Rep*. 2018;**8**(1):13803. doi: 10.1038/s41598-018-31940-2. [PubMed: 30218059]. [PubMed Central: PMC6138673].
33. Muthuchellappan R, V JR, Ganne S, K T, Jacob A, G S, et al. Correlation between time lag of arterial-plethysmographic waveforms and systemic vascular resistance: a prospective study. *J Med Eng Technol*. 2018;**42**(1):18–25. doi: 10.1080/03091902.2017.1409817. [PubMed: 29251031].
34. Yadav SK, Mishra S, Mishra B. Eudragit-based nanosuspension of poorly water-soluble drug: formulation and in vitro-in vivo evaluation. *AAPS PharmSciTech*. 2012;**13**(4):1031–44. doi: 10.1208/s12249-012-9833-0. [PubMed: 22893314]. [PubMed Central: PMC3513456].

35. Mohyeldin SM, Mehanna MM, Elgindy NA. The relevancy of controlled nanocrystallization on rifampicin characteristics and cytotoxicity. *Int J Nanomedicine*. 2016;**11**:2209–22. doi: 10.2147/IJN.S94089. [PubMed: 27274244]. [PubMed Central: PMC4876945].
36. Singare DS, Marella S, Gowthamrajan K, Kulkarni GT, Vooturi R, Rao PS. Optimization of formulation and process variable of nanosuspension: An industrial perspective. *Int J Pharm*. 2010;**402**(1-2):213–20. doi: 10.1016/j.ijpharm.2010.09.041. [PubMed: 20933066].
37. Moorthi C, Krishnan K, Manavalan R, Kathiresan K. Preparation and characterization of curcumin-piperine dual drug loaded nanoparticles. *Asian Pac J Trop Biomed*. 2012;**2**(11):841–8. doi: 10.1016/S2221-1691(12)60241-X. [PubMed: 23569859]. [PubMed Central: PMC3609247].
38. Abdelbary AA, Li X, El-Nabarawi M, Elassasy A, Jasti B. Effect of fixed aqueous layer thickness of polymeric stabilizers on zeta potential and stability of aripiprazole nanosuspensions. *Pharm Dev Technol*. 2013;**18**(3):730–5. doi: 10.3109/10837450.2012.727001. [PubMed: 23033924].
39. Ali HS, York P, Blagden N. Preparation of hydrocortisone nanosuspension through a bottom-up nanoprecipitation technique using microfluidic reactors. *Int J Pharm*. 2009;**375**(1-2):107–13. doi: 10.1016/j.ijpharm.2009.03.029. [PubMed: 19481696].
40. Galperin A, Margel D, Baniel J, Dank G, Biton H, Margel S. Radiopaque iodinated polymeric nanoparticles for X-ray imaging applications. *Biomaterials*. 2007;**28**(30):4461–8. doi: 10.1016/j.biomaterials.2007.06.032. [PubMed: 17644171].
41. Bai MY, Moran CH, Zhang L, Liu C, Zhang Y, Wang LV, et al. A Facile and General Method for the Encapsulation of Different Types of Imaging Contrast Agents Within Micrometer-Sized Polymer Beads. *Adv Funct Mater*. 2012;**22**(4):764–70. doi: 10.1002/adfm.201102582. [PubMed: 31866803]. [PubMed Central: PMC6924621].
42. Andreucci M, Faga T, Pisani A, Sabbatini M, Russo D, Michael A. Prevention of contrast-induced nephropathy through a knowledge of its pathogenesis and risk factors. *ScientificWorldJournal*. 2014;**2014**:823169. doi: 10.1155/2014/823169. [PubMed: 25525625]. [PubMed Central: PMC4266998].
43. Seeliger E, Flemming B, Wronski T, Ladwig M, Arakelyan K, Godes M, et al. Viscosity of contrast media perturbs renal hemodynamics. *J Am Soc Nephrol*. 2007;**18**(11):2912–20. doi: 10.1681/ASN.2006111216. [PubMed: 17942967].
44. Jensen H, Doughty RW, Grant D, Myhre O. The effects of the iodinated X-ray contrast media iodixanol, iohexol, iopromide, and ioversol on the rat kidney epithelial cell line NRK 52-E. *Ren Fail*. 2011;**33**(4):426–33. doi: 10.3109/0886022X.2011.568146. [PubMed: 21529272].
45. Andersen KJ, Vik H, Eikesdal HP, Christensen EI. Effects of contrast media on renal epithelial cells in culture. *Acta Radiol Suppl*. 1995;**399**:213–8. doi: 10.1177/02841851950360s39926. [PubMed: 8610519].
46. Jeong CH, Machek EJ, Shakeri M, Duirk SE, Ternes TA, Richardson SD, et al. The impact of iodinated X-ray contrast agents on formation and toxicity of disinfection by-products in drinking water. *J Environ Sci (China)*. 2017;**58**:173–82. doi: 10.1016/j.jes.2017.03.032. [PubMed: 28774606].
47. Thurman JM, Serkova NJ. Nanosized contrast agents to noninvasively detect kidney inflammation by magnetic resonance imaging. *Adv Chronic Kidney Dis*. 2013;**20**(6):488–99. doi: 10.1053/j.ackd.2013.06.001. [PubMed: 24206601]. [PubMed Central: PMC3828648].